JOURNAL OF APPLIED ELECTROCHEMISTRY 18 (1988) 532–537

Influence of oxide bond energies on the kinetics of chemical dissolution of anodic oxides on valve metals

A. G. GAD-ALLAH, H. A. ABD EL-RAHMAN, M. M. ABOU-ROMIA

Chemistry Department, Faculty of Science, University of Cairo, Giza, Egypt

Received 16 August 1987; revised 21 January 1988

The influence of M–O bond energies on the kinetics of the chemical dissolution of anodic oxide films on valve metals was analysed and the different profiles of atomic defects in these oxides were deduced. Four different equations describing the dissolution behaviour of such oxides were derived and the respective examples justifying each equation were also introduced. For many oxides, M–O bond energy was found to vary linearly with the activation energy of the dissolution. It was also found that the dissolution rate increases with increase of the initial thickness of the oxide. The dissolution processes were followed by using potential and capacitance measurements.

1. Introduction

For electrode processes such as the hydrogen and oxygen evolution reactions, M–H and M–OH bond energies, respectively, have been related quantitatively to the electrode kinetic parameters [1, 2] of the corresponding metals. M–O bond energies of anodic oxides on valve metals have also been related to the kinetic parameters of their growth under constant current density [3]. For several valve metal oxides, the various fundamental properties, e.g. m.p., b.p., were found to increase systematically with increase in M–O bond energy [4]. These oxides were assumed to be predominantly covalent [5] and their activation energies for the formation and diffusion of point defects (EDF) would be expected to increase with increasing M–O bond energy [4].

In the absence of transport phenomena, the kinetics of chemical dissolution of anodic oxides, as heterogeneous reactions, are governed mainly by disruption of the primary aggregation forces in the solid (i.e. M–O bonds). On oxides with high bond energies, chemical bonding disruption occurs at sites where defects are present. From the dependency of the dissolution rate on the instantaneous surface defect concentration, Hefny *et al.* [6] deduced three different profiles of defects in anodic films depending on the magnitude of the M–O bond energies (cf. Fig. 1A). The equations describing the dissolution kinetics were as follows [6]:

$$x = x_0 \exp(-K_1^L K_2^L t) \quad (1a)$$

$$x^2 = x_0^2 - 2K_1^M K_2^M t \quad (1b)$$

$$x = x_0 - K_1^H K_2^H t \quad (1c)$$

where x and x_0 are the oxide thickness at dissolution times of t and zero, respectively; K_1^L, K_1^M, K_1^H are constants depending on the dissolving solutions and K_2^L, K_2^M, K_2^H are constants depending on the nature of the oxides and their formation conditions. Although the previous treatment [6] succeeds in describing the dissolution behaviour of some oxides, it fails in other cases [7–9].

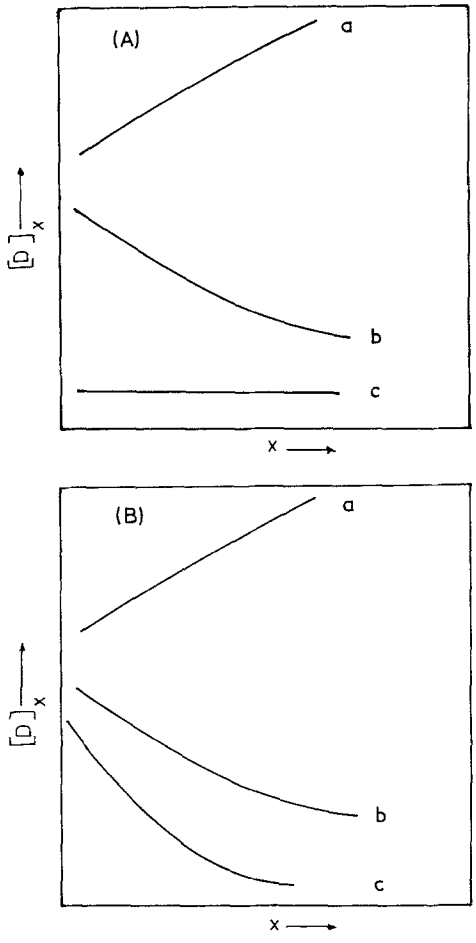

Fig. 1. Variation of the defect concentration, $[D]_x$, with the oxide film thickness. (A) Oxides having (a) low, (b) moderate and (c) high bond energies according to [6]; (B) oxides having (a) low, (b) moderate and (c) high bond energies according to the present authors.

In this paper, the previous treatment will be modified to account for the different dissolution behaviour of anodic oxides. New illustrative examples will be also introduced.

0021-891X/88 $03.00 + .12

Following Fig. 1B, the dissolution kinetics are classified into four types.

1.1. *Dissolution of oxides having low M–O bond energies (class a)*

It is assumed that the rate of dissolution, $-dx/dt$, depends on the instantaneous surface defect concentration, $[D]_x$, i.e.

$$-dx/dt = K_1^{\prime}[D]_x \quad (2)$$

where $K_1^{\prime}$ is a constant which depends on the dissolving solution. For class a oxides, it is also assumed that

$$[D]_x = K_2^{\mathrm{L}} x \quad (3)$$

Combining Equations 2 and 3 gives

$$-dx/dt = K_1^{\mathrm{L}} K_2^{\mathrm{L}} x \quad (4)$$

Integration of Equation 4 gives

$$x = x_0 \exp(-K_1^{\mathrm{L}} K_2^{\mathrm{L}} t) \quad (5)$$

or

$$\log x = \log x_0 - (K_1^{\mathrm{L}} K_2^{\mathrm{L}}/2.303)\, t \quad (6)$$

1.2. *Dissolution of oxides having moderate M–O bond energies (class b)*

Here

$$[D]_x = K_2^{\mathrm{M}}/x \quad (7)$$

Combining Equations 2 and 7 gives

$$-dx/dt = K_1^{\mathrm{M}} K_2^{\mathrm{M}}/x \quad (8)$$

Integration of the above equation gives

$$x^2 = x_0^2 - K_1^{\mathrm{M}} K_2^{\mathrm{M}} t \quad (9)$$

or

$$(x - x_0)(x + x_0) = -(K_1^{\mathrm{M}} K_2^{\mathrm{M}} t)^{1/2} (K_1^{\mathrm{M}} K_2^{\mathrm{M}} t)^{1/2} \quad (10)$$

Splitting the above equation gives

$$(x - x_0) = -(K_1^{\mathrm{M}} K_2^{\mathrm{M}})^{1/2} t^{1/2} \quad (11)$$

and

$$(x + x_0) = (K_1^{\mathrm{M}} K_2^{\mathrm{M}})^{1/2} t^{1/2} \quad (12)$$

Equation 11 is assumed to govern the kinetics of dissolution of oxides in this class.

1.3. *Dissolution of oxides having high M–O bond energies (class d)*

In this case

$$[D]_x = K_2^{\mathrm{H}} \exp^{(-mx)} \quad (13)$$

where m is a constant. According to Equation 13, the concentration of atomic defects is assumed to decrease exponentially with increase of the oxide thickness which necessitates the blocking of the defects homogeneously as the oxide grows. Combining Equations 2 and 13 gives

$$-dx/dt = K_1^{\mathrm{H}} K_2^{\mathrm{H}} \exp^{(-mx)} \quad (14)$$

Integration of Equation 14 gives

$$x = \frac{2.303}{m} \log(1/t^0) - \frac{2.303}{m} \log(t + t^0) \quad (15)$$

where $t^0 = 1/mK_1^{\mathrm{H}} K_2^{\mathrm{H}}$.

1.4. *Dissolution of oxides under highly aggressive conditions*

In this case, the rate of dissolution is independent of the defect concentration, hence

$$-dx/dt = K^{\mathrm{A}} \quad (16)$$

where K^{A} is a constant. Integration of the above equation gives

$$x = x_0 - K^{\mathrm{A}} t \quad (17)$$

If the thickness of the oxides are expressed in terms of reciprocal capacitances, C_{m}^{-1}, Equations 6, 11, 15 and 17 become

$$\log C_{\mathrm{m}}^{-1} = \log 1/C_{\mathrm{m}}^0 - K_{\mathrm{d}}^{\mathrm{L}} t \quad (18)$$

$$C_{\mathrm{m}}^{-1} = 1/C_{\mathrm{m}}^0 - K_{\mathrm{d}}^{\mathrm{M}} t^{1/2} \quad (19)$$

$$C_{\mathrm{m}}^{-1} = \text{const.} - K_{\mathrm{d}}^{\mathrm{H}} \log(t + t^0) \quad (20)$$

$$C_{\mathrm{m}}^{-1} = 1/C_{\mathrm{m}}^0 - K_{\mathrm{d}}^{\mathrm{A}} t \quad (21)$$

where $K_{\mathrm{d}}^{\mathrm{L}}$, $K_{\mathrm{d}}^{\mathrm{M}}$, $K_{\mathrm{d}}^{\mathrm{H}}$ and $K_{\mathrm{d}}^{\mathrm{A}}$ are constants.

2. Experimental details

The electrodes used were in the form of rods having the specifications given in Table 1. The electrode preparation, the electrolytic cell, the electric circuit and details of the experimental procedure were described previously [10, 11]. The electrode surface was abraded down to 4/0 emery paper, then the electrode was immersed in the anodizing solution (AS). The electrode was anodized at a constant anodizing current density (ACD) until the specified formation voltage (F_{v}) was reached, then the current was interrupted and the electrode, after being washed quickly and gently with triply distilled water, was transferred to the dissolving solution (DS). Immediately, the electrode capacitance, C_{m}, was measured as a function of time at 1 kHz. All solutions used were prepared from AnalaR grade chemicals and triply distilled water. All potentials were measured versus a saturated calomel electrode (SCE) at 30° C.

The dissolution processes are usually accompanied

Table 1. Specifications of the electrodes

Electrode	*Area (cm²)*	*Purity*	*Source*
Hf	0.035	99.9%	Koch Light Lab. Ltd, UK
Al	0.125	Spec. pure	Johnson-Matthey, UK
W	0.125	Spec. pure	Johnson-Matthey, UK
Mo	0.125	Spec. pure	Johnson-Matthey, UK
Ta	0.169	Spec. pure	Johnson-Matthey, UK
Zr	0.096	Spec. pure	Johnson-Matthey, UK
Ti	0.071	Spec. pure	Johnson-Matthey, UK

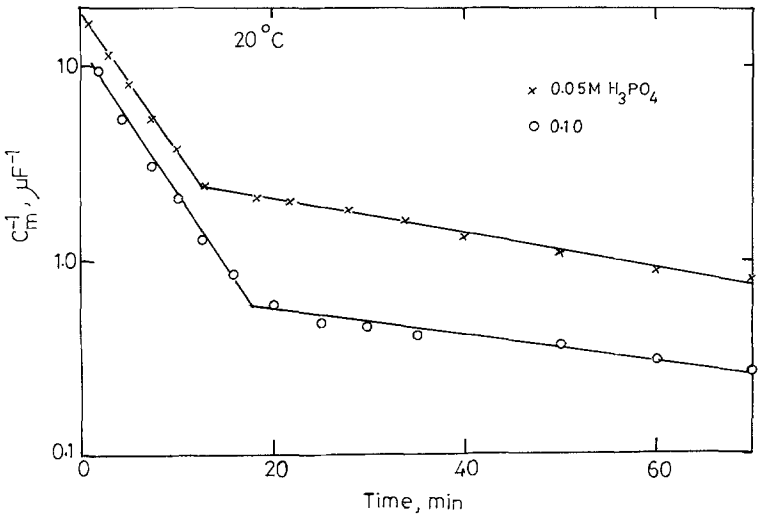

Fig. 2. Variation of logarithm of the reciprocal capacitance, C_m^{-1}, of anodized tungsten electrodes with time in solutions of (○) 0.1 M H_3PO_4 and (×) 0.05 M H_3PO_4; F_v = 70 V, ACD = 0.8 mA cm^{-2} and AS was 0.1 M H_3PO_4 acid.

by: (i) an increase in capacitance; (ii) a decrease in resistance; (iii) a shift of corrosion potential towards more negative values; (iv) a change in the interference colours with time [7–9, 11–13]. Assuming that the dielectric constants of the oxides are invariable during the dissolution processes, the measured capacitance is proportional to the thickness of the remaining film [7–9, 11–15].

3. Results and discussion

The dissolution behaviour of some valve metal oxides in alkaline solutions is shown in Figs 2–8. As can be seen, the anodic oxide on W dissolves according to Equation 18. The oxides on Ta, Zr, Ti and Al dissolve according to Equation 19. The oxide on Hf was subject to dissolution according to Equation 20 while that on Mo dissolves following Equation 21. The values of M–O bond energies of some valve metal oxides, being calculated from the appropriate thermodynamic data, are given, together with the theoretically derived and the experimentally observed equations, in Table 2. From this table it may be seen that the assumptions made in deriving the dissolution Equations 18–21 seem to be valid. The changes in gradient in some dissolution curves are attributed to the duplex nature of the oxides [6, 12, 13, 16–18] or the contribution of transport processes [19].

The present classification can account for the presence of two dissolution equations of some anodic oxides, one of which is always Equation 21. As examples: (i) WO_3 was found to dissolve in H_2SO_4 acid solutions [11] according to Equation 18, while it dissolved in phosphate solutions following Equation 21; (ii) sulphuric acid anodized aluminium was found to dissolve in H_2SO_4 and HCl solutions [20] according to Equation 21, while phosphoric acid anodized aluminium [12] dissolved following Equation 19. Actually, these findings reflect the modes of dissolution of anodic oxides either normally, i.e. controlled by the oxide properties, or under highly aggressive conditions, i.e. independent of the oxide properties. The aggressive

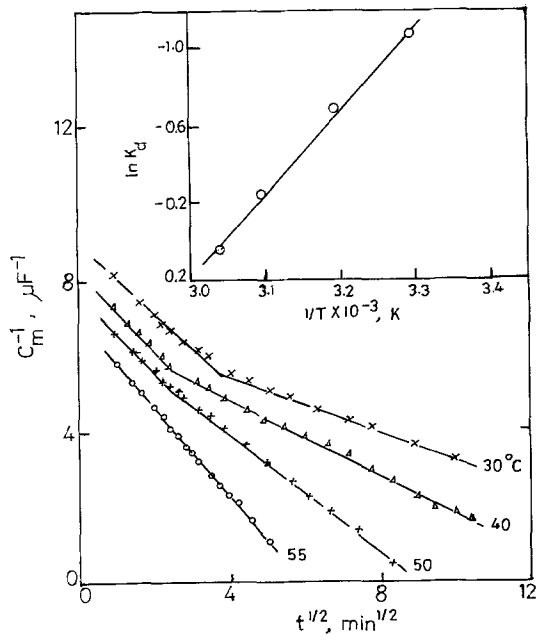

Fig. 3. (A) Variation of reciprocal capacitance, C_m^{-1}, of anodized titanium electrodes with the square root of time in 2 M NaOH solutions; F_v = 15 V, ACD = 5 mA cm^{-2} and AS was 0.01 M K_2HPO_4. (B) Arrhenius plot.

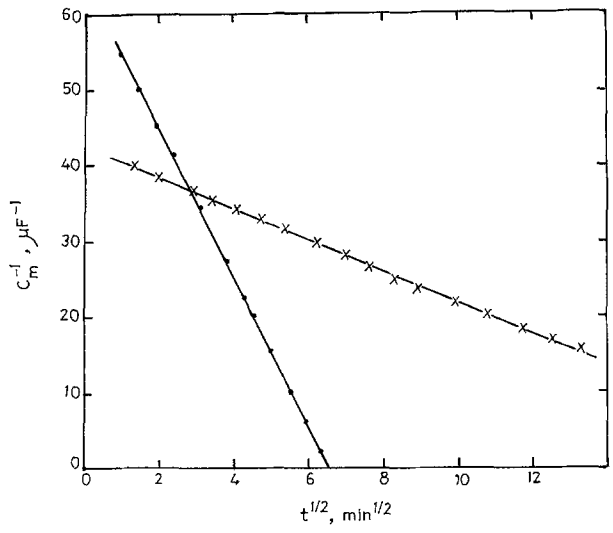

Fig. 4. Variation of reciprocal capacitance, C_m^{-1}, of anodized aluminium electrodes with the square root of time in stirred solutions of (●) 0.01 N NaOH and (×) 2.75 N H_2SO_4; F_v = 100 V, ACD = 8 mA cm^{-2} and AS was 0.1 M potassium tartrate.

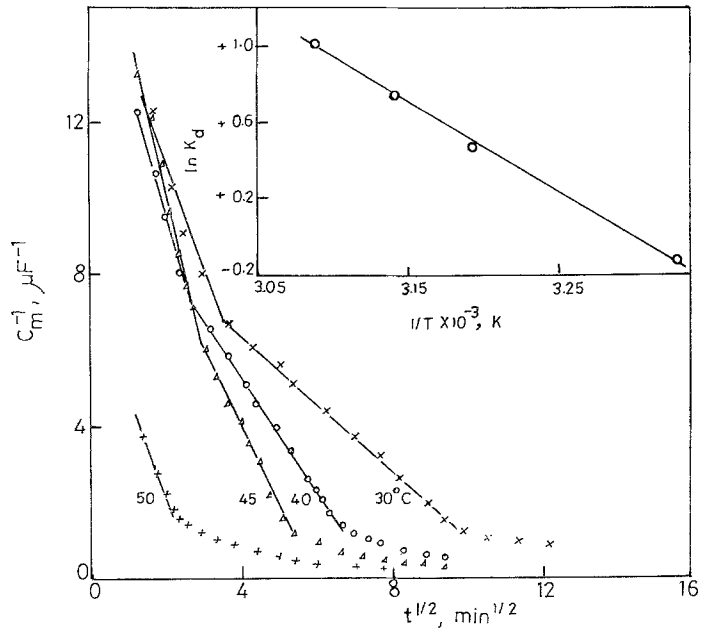

Fig. 5. (A) Variation of reciprocal capacitance, C_m^{-1}, of anodized zirconium electrodes with the square root of time in 4 M NaOH solutions; F_v = 80 V, ACD = 1 mA cm^{-2} and AS was 0.01 M H_2SO_4 acid. (B) Arrhenius plot.

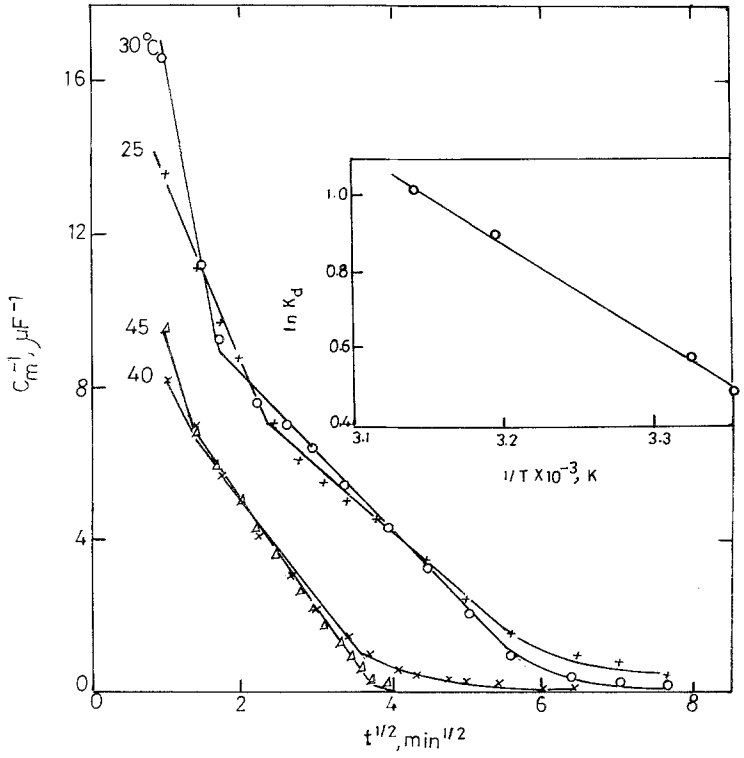

Fig. 6. (A) Variation of reciprocal capacitance, C_m^{-1}, of anodized tantalum electrodes with the square root of time in 7 M NaOH solutions; F_v = 100 V, ACD = 5 mA cm^{-2} and AS was 0.01 M H_2SO_4 acid. (B) Arrhenius plot.

conditions may be the formation electrolyte, the anodizing current, the dissolving electrolyte and the formation and dissolution temperatures.

As a consequence of the dependence of the dissolution kinetics of anodic oxides on M–O bond energies, it might be expected that the activation energies of dissolution, ΔE_a, will also be dependent on them. The values of ΔE_a were estimated from Arrhenius plots [12, 21] and represented graphically versus the corresponding M–O bond energy in Fig. 9. Except for the oxide on Zr, which shows some anomalous characteristics of a fundamental nature in its kinetic behaviour [3, 22], an almost linear relation between ΔE_a and bond energy can be seen. This relation supports the assumptions of the existence of an influence of M–O bond energies on the kinetics of dissolution of anodic oxide films.

Table 2. M–O bond energies and numbers of theoretically expected and experimentally observed equations

Oxide	*Bond energy (eV)*	*Dissolution equation*	
		Theoretical	*Experimental*
Sb_2O_3	3.91	18	18(13)
WO_3	4.76	18	18
Nb_2O_5	5.29	—	21(9)
Ta_2O_5	5.34	19	19
TiO_2	5.42	19	19
Al_2O_3	5.73	19	19
ZrO_2	6.16	19	19
HfO_2	6.42	20	20
MoO_2	—	—	21

All values of bond energies, except that of Sb_2O_3, were taken from Ref. [3], that of Sb_2O_3 was taken from Ref. [6].
The numbers in the parentheses refer to the source reference.

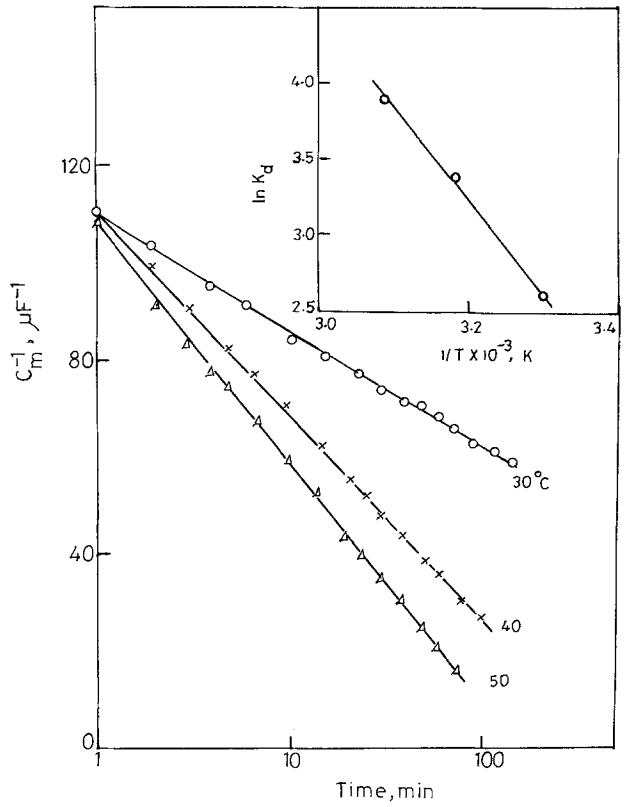

Fig. 7. (A) Variation of reciprocal capacitance, C_m^{-1}, of anodized hafnium electrodes with logarithm of time in 9 M NaOH solutions; F_v = 100 V, ACD = 2.8 mA cm^{-2} and AS was 0.5 M H_2SO_4 acid. (B) Arrhenius plot.

Usually, thick oxide films dissolve more rapidly than thin ones [7, 8, 18, 19, 23]. Figure 10 shows the linear variation of the dissolution rate constant with the initial film thickness (in terms of F_v) on a double logarithmic scale. These findings do not contradict the assumptions proposed in deriving Equations 19 and 20 where it has been assumed that the rate of dissolution decreases as the thickness increases. The increase of the dissolution rate with increase of the initial thickness is attributed, simply, to the increase of the exposed surface area to the dissolving solution.

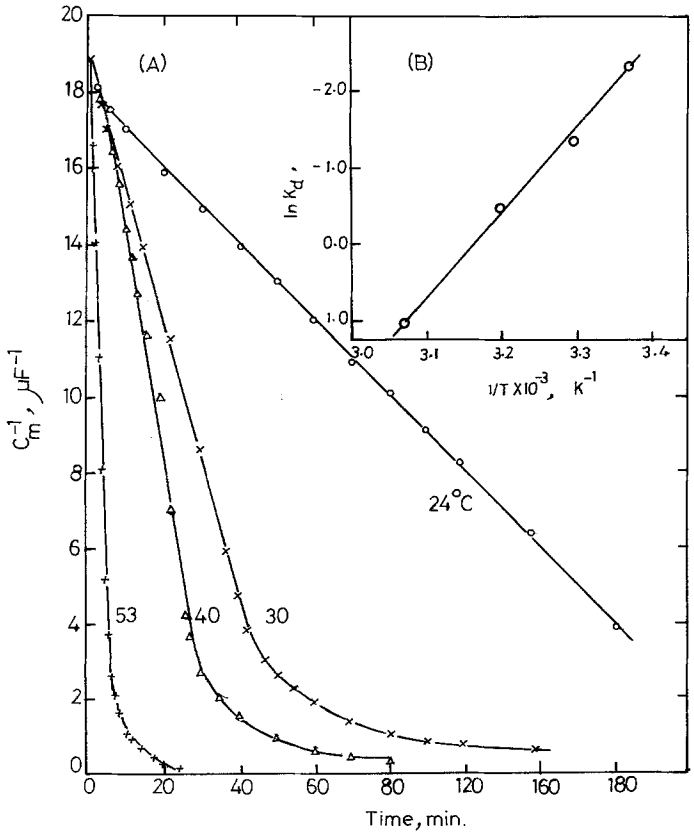

Fig. 8. (A) Variation of reciprocal capacitance, C_m^{-1}, of anodized molybdenum electrodes with time in 9 M NaOH solutions; F_v = 50 V, ACD = 8 mA cm^{-2} and AS was 0.005 M H_2SO_4 acid. (B) Arrhenius plot.

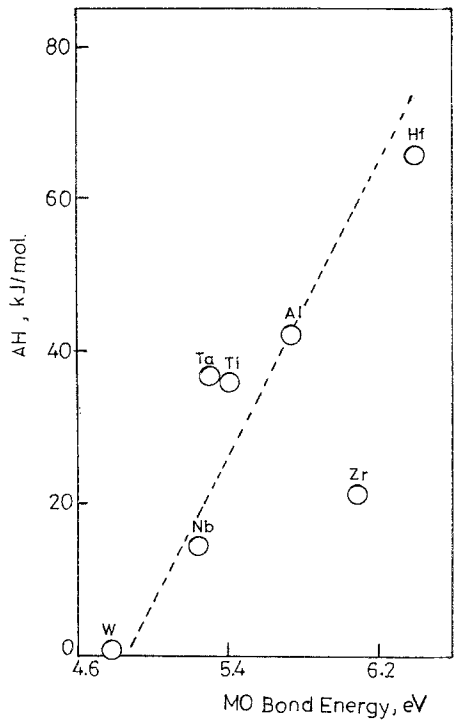

Fig. 9. Variation of the activation energy of oxide dissolution, ΔE_a, in alkaline solutions with M–O bond energy.

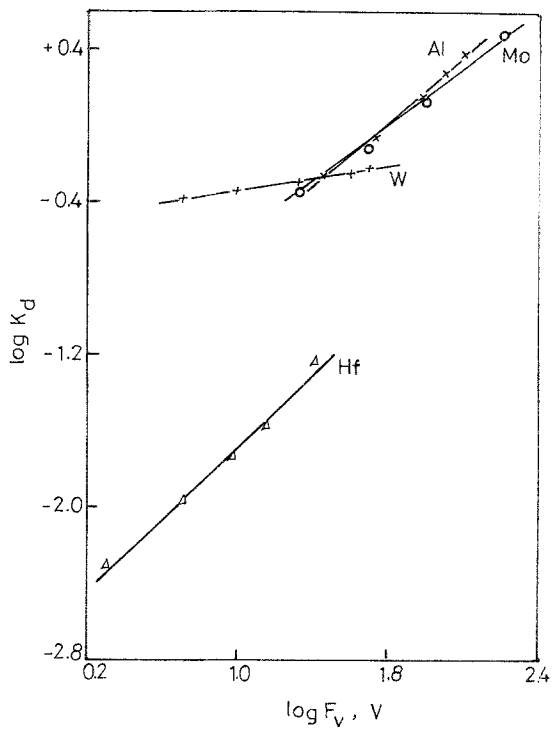

Fig. 10. Variation of the logarithm of dissolution rate, log K_d, with logarithm of the formation voltage, F_v.

References

[1] B. E. Conway and J. O'M. Bockris, *J. Chem. Phys.* **26** (1957) 532.
[2] P. Ruetschi and P. Delahay, *ibid.* **23** (1955) 556.
[3] A. K. Vijh, *J. Electrochem. Soc.* **116** (1969) 972.
[4] Idem, *ibid.* **116** (1969) 353; **115** (1968) 1096.
[5] A. Vorobe'v, *Russ. Chem. Rev.* **36** (1967) 440, English trans., Consultants Bureau, New York.
[6] M. M. Hefny, A. S. Mogoda and M. S. El-Basiouny, *Br. Corros. J.* **21** (1986) 109.
[7] M. M. Hefny, M. S. El-Basiouny, A. G. Gad-Allah and S. A. Salih, *Electrochim. Acta* **28**, (1983) 1811.
[8] A. S. Mogoda, M.Sc. Thesis, Cairo University (1982).
[9] W. A. Badawy, A. G. Gad-Allah and H. H. Rehan, *J. Appl. Electrochem.* **17** (1987) 559.
[10] W. A. Badawy, A. G. Gad-Allah, H. A. Abd El-Rahman and M. M. Abou-Romia, *Surf. Coat. Technol.* **27** (1986) 187.
[11] M. S. El-Basiouny, S. A. Hassan and M. M. Hefny, *Corros. Sci.* **20** (1980) 909.
[12] W. A. Badawy, M. S. El-Basiouny and M. M. Ibrahim, *Indian J. Tech.* **24** (1986) 1.
[13] M. M. Hefny, W. A. Badawy, A. S. Mogoda and M. S. El-Basiouny, *Electrochim. Acta* **30** (1985) 1017.
[14] L. Young, 'Anodic Oxide Films', Academic Press, London (1960).
[15] Chr. Bartels, J. W. Schultze, U. Stimmig and M. A. Habib, *Electrochim. Acta* **27** (1980) 129.
[16] M. M. Hefny, M. S. El-Basiouny and A. S. Mogoda, *Corrosion* **39** (1983) 266.
[17] M. S. El-Basiouny, A. A. Mazhar, F. El-Taib Heakal and M. A. Ameer, *J. Electroanal. Chem.* **147** (1983) 181.
[18] M. S. El-Basiouny and A. A. Mazhar, *Corrosion* **38** (1982) 5.
[19] A. G. Gad-Allah and H. A. Abd El-Rahman, *Corros. Sci.* in course of publication.
[20] J. W. Diggle, T. C. Dowie and C. W. Goulding, *Electrochim. Acta* **15** (1970) 1079.
[21] J. O'M. Bockris and E. C. Potter, *J. Chem. Phys.* **20** (1952) 614.
[22] M. J. Dignam, *J. Electrochem. Soc.* **42** (1964) 1155.
[23] R. S. Alwitt and R. G. Hill, *ibid.* **112** (1965) 974.